Review

Polymer Nanocomposites Containing Carbon Nanotubes

Mohammad Moniruzzaman and Karen I. Winey*

*Department of Materials Science and Engineering, University of Pennsylvania,
Philadelphia, Pennsylvania 19104*

Received April 1, 2006; Revised Manuscript Received May 18, 2006

ABSTRACT: We review the present state of polymer nanocomposites research in which the fillers are single-wall or multiwall carbon nanotubes. By way of background we provide a brief synopsis about carbon nanotube materials and their suspensions. We summarize and critique various nanotube/polymer composite fabrication methods including solution mixing, melt mixing, and in situ polymerization with a particular emphasis on evaluating the dispersion state of the nanotubes. We discuss mechanical, electrical, rheological, thermal, and flammability properties separately and how these physical properties depend on the size, aspect ratio, loading, dispersion state, and alignment of nanotubes within polymer nanocomposites. Finally, we summarize the current challenges to and opportunities for efficiently translating the extraordinary properties of carbon nanotubes to polymer matrices in hopes of facilitating progress in this emerging area.

1. Introduction

Carbon nanotubes (CNT) were first reported by Iijima[1] in 1991, and the first polymer nanocomposites using carbon nanotubes as a filler were reported in 1994 by Ajayan et al.[2] Earlier nanocomposites used nanoscale fillers such as carbon blacks, silicas, clays, and carbon nanofibers (CNF) to improve the mechanical, electrical, and thermal properties of polymers. Carbon nanotubes possess high flexibility,[3] low mass density,[4] and large aspect ratio (typically ca. 300−1000). CNT have a unique combination of mechanical, electrical, and thermal properties that make nanotubes excellent candidates to substitute or complement the conventional nanofillers in the fabrication of multifunctional polymer nanocomposites. Some nanotubes are stronger than steel, lighter than aluminum, and more conductive than copper. For example, theoretical and experimental results on individual single-wall carbon nanotubes (SWNT) show extremely high tensile modulus[5] (640 GPa to 1 TPa) and tensile strength[6] (150−180 GPa). Depending on their structural parameters, SWNT can be metallic or semiconducting, which further expands their range of applications. Because of the nearly one-dimensional electronic structures, metallic nanotubes can transport electrons over long tube lengths without significant scattering (electronic mean free path for metallic SWNT is on the order of several microns[7]). Similarly, SWNT exhibit large phonon mean free path lengths that result in high thermal conductivity (theoretically[8] >6000 W/(m K)). Because of these extraordinary properties of isolated carbon nanotubes, great enthusiasm exists among researchers around the world as they explore the immense potential of these nanofillers. The level of activity is illustrated by the number of journal articles and patents published within a short period of time (Figure 1). These documents address various aspects of nanotube produc-

tion, purification, suspension, filling, functionalization, and applications as well as the fabrication and characterization of polymer nanocomposites with various types of nanotubes.

Indicative of an emerging technology, there are only a few nanotube-based commercial products in the market at present. As a matter of fact, the only major commercial product based on nanotubes in the market for the past decade has been a nanotube/plastic composite with improved electrical conductivity that facilitates electrostatic coating and is marketed by Hyperion Catalysis International, Inc. To close the gap between the high expectations and technological achievements with CNT composites, one must wrestle with the "less than ideal" and inconsistent nature of nanotubes. All known preparations of CNT give mixtures of nanotube chiralities, diameters, and lengths along with different amount of impurities and structural defects. These parameters vary significantly both within a sample and between samples from different batches and laboratories. Thus, it is very difficult to conduct reproducible control experiments with these inconsistent nanofillers and virtually impossible to compare results between different researchers. Another great challenge in nanotube/polymer composites is the efficient translation of nanotube properties both into the polymer matrix and between nanotubes. Those with clever schemes for fabricating nanotube/polymer composites are addressing these challenges most effectively. While significant insights have been achieved, there are still many unresolved issues that need to be addressed theoretically and experimentally to harness the maximum benefits from carbon nanotubes in polymer composite systems. In this review we will discuss the progress, remaining challenges, and future directions of the nanotubes/polymer composite research. Several review articles[9−13] have been published recently on various aspects of nanotube/polymer composites, but this article is a critical review of the most significant results in the field.

* Corresponding author: Tel +1 215 8980593; Fax +1 215 5732128; e-mail winey@seas.upenn.edu.

Figure 1. Number of published journal articles and issued and pending patents on nanotubes and nanotube/polymer composites as a function of year.

Mohammad Moniruzzaman received his B.Sc. and M.Sc. (with Prof. Farida Akhtar) in Chemistry from Jahangirnagar University, Bangladesh. He earned his Ph.D. in Materials Chemistry with Prof. P. R. Sundararajan at Carleton University, Canada. He is presently a postdoctoral fellow with Prof. Karen I. Winey at the University of Pennsylvania. His postdoctoral research focuses on the fabrication and characterization of polymer nanocomposites containing carbon nanotubes. He was a recipient of Ontario Graduate Scholarship in Science and Technology (OGSST) and presently has an NSERC postdoctoral fellowship from the Natural Science and Engineering Research Council of Canada.

Figure 2. Schematic diagram showing how a hexagonal sheet of graphene is "rolled" to form a carbon nanotube. The rolling shown in the diagram will form a (3,2) nanotube. Reprinted with permission from ref 16. Copyright 2001 Elsevier.
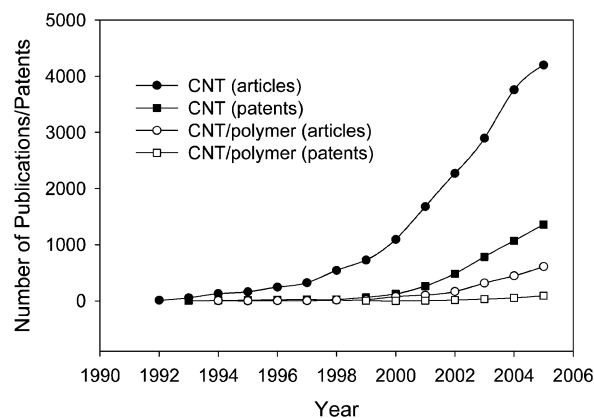
Professor Karen I. Winey is currently a Professor of Materials Science and Engineering, as well as Chemical and Biomolecular Engineering, at the University of Pennsylvania. Winey earned a B.S. in Materials Science and Engineering from Cornell University and a M.S. and Ph.D. in Polymer Science and Engineering from the University of Massachusetts under the direction of Prof. Edwin L. Thomas. After spending 17 months as a Postdoctoral Member of Technical Staff at AT&T Bell Laboratories, she joined the University of Pennsylvania in 1992. Winey received a National Science Foundation Young Investigator Award in 1994 and became a Fellow of the American Physical Society in 2003. Her research expertise in polymeric materials includes ion-containing polymers, block copolymers, and nanotube−polymer composites with specialties in materials processing, morphological characterization, and structure−properties relationships.

2. Carbon Nanotubes

Before exploring the various aspects of nanotube/polymer composite systems, we first describe the carbon nanotubes. Nanotubes come in different types, and they vary significantly depending on the syntheses procedures. This section contains a brief introduction to nanotubes, sources of nanotubes, and some fundamental properties of nanotubes that are critical to understanding nanotube/polymer composites.

Carbon nanotubes are long cylinders of covalently bonded carbon atoms. The ends of the cylinders may or may not be capped by hemifullerenes. There are two basic types of CNT: single-wall carbon nanotubes (SWNT) and multiwall carbon nanotubes (MWNT). SWNT can be considered as a single

graphene sheet (graphene is a monolayer of sp^2-bonded carbon atoms) rolled into a seamless cylinder. The carbon atoms in the cylinder have partial sp^3 character that increases as the radius of curvature of the cylinder decreases. MWNT consist of nested graphene cylinders coaxially arranged around a central hollow core with interlayer separations of ∼0.34 nm, indicative of the interplane spacing of graphite.[14] A special case of MWNT is double-wall nanotubes (DWNT) that consist of two concentric graphene cylinders. DWNT are expected to exhibit higher flexural modulus than SWNT due to the two walls and higher toughness than regular MWNT due to their smaller size.[15] The nanotubes can be filled with foreign elements or compounds, e.g., with C_{60} molecules, to produce hybrid nanomaterials which possess unique intrinsic properties, such as transport properties.[15] These hybrid nanomaterials currently have limited availability, but as production increases this might be a new opportunity for polymer nanocomposites.

The various ways of rolling graphene into tubes are described by the tube chirality (or helicity or wrapping) as defined by the circumferential vector, $\vec{C}_h = n\vec{a}_1 + m\vec{a}_2$ (Figure 2), where the integers (n, m) are the number of steps along the unit vectors $(\vec{a}_1$ and $\vec{a}_2)$ of the hexagonal lattice.[16] Using this (n, m) naming scheme, the three types of orientation of the carbon atoms around the nanotube circumference are specified as arm chair $(n = m)$, zigzag $(n = 0$ or $m = 0)$, or chiral (all others). The chirality of nanotubes has significant impact on its transport properties, particularly the electronic properties. All armchair SWNT are metallic with a band gap of 0 eV. SWNT with $n - m = 3i$ (i being an integer and $\neq 0$) are semimetallic with a

band gap on the order of a few meV, while SWNT with $n - m \neq 3i$ are semiconductors with a band gap of ca. $0.5-1$ eV.[17] Each MWNT contains a variety of tube chiralities, so their physical properties are more complicated to predict.

Presently, MWNT and SWNT are mainly produced by three techniques, each having their own nuances: arc discharge, laser ablation, and chemical vapor decomposition (CVD). A number of reviews[14,16] are available on these production techniques. Arc discharge and laser ablation methods involve the condensation of hot gaseous carbon atoms generated from the evaporation of solid carbon. In CVD a gaseous carbon source (hydrocarbon, CO) is decomposed catalytically, and the nanotubes are deposited on a substrate or grow from a substrate. Compared with arc and laser methods, CVD might offer more control over the length and structure of the produced nanotubes, and the process appears scalable to industrial quantities. In fact, Hyperion Catalysis International Inc. produces MWNT (trade name FIBRIL nanotubes) using a CVD method. Carbon Nanotechnology Inc. (Houston, TX) produces SWNT using a floating catalyst CVD method, known as high-pressure catalytic decomposition of carbon monoxide or HiPco.

As mentioned earlier, at present, all known preparations of CNT give mixtures of nanotube chiralities, diameters, and lengths along with different amount and type of impurities. This CNT heterogeneity has important implications when purifying carbon nanotubes and preparing nanotube/polymer composites. For example, smaller diameter SWNT are more susceptible to both thermal degradation and chemical functionalization, such that the diameter distribution can be altered between SWNT synthesis and nanotube/polymer composite fabrication. A typical SWNT average diameter is $\sim 1.2-1.4$ nm, and the minimum diameter of a stable free-standing SWNT is limited by curvature induced strain to ~ 0.4 nm.[18] The variation in SWNT diameter is also illustrated by the coexistence of various wrappings (n, m), where the circumferential vectors are used to calculate the nanotube diameters. MWNT can have diameters from several nanometers to several hundred nanometers. The reported lengths of nanotubes range from several tens of nanometers to several centimeters.[19] The properties of the nanotube/polymer composites will vary significantly depending on the distribution of the type, diameter, and length of the nanotubes.

3. Nanotube Suspensions

A true solvent for pristine nanotubes is yet to be found. The high aspect ratio of the nanotubes coupled with a strong intrinsic van der Waals attraction between nanotubes combine to produce ropes and bundles of CNT, particularly in SWNT where the attractive force is ~ 0.5 eV per nanometer of nanotube-to-nanotube contact.[17] Ropes refer to collections of SWNT that are sufficiently uniform in diameter to form a hexagonal lattice while bundles are noncrystalline collections of SWNT or MWNT. With the aid of ultrasonication, nanotubes can be moderately dispersed in some solvents, e.g., in dimethylformamide and dichlorobenzene, to produce nanotube suspensions. Understanding nanotube suspensions is vital to controlling various solvent-based processes (phase separation, chemical derivatization, etc.) associated with preparing nanotube/polymer composites because the initial nanotube dispersion can impact the nanotube dispersion in the polymer matrix.

Three important questions arise regarding nanotube suspensions. What is the size distribution of suspended nanotube objects? This is critical because, for example, isolated tubes facilitate extensive chemical derivitatization in suspension and provide the highest interfacial area for stress transfer to the
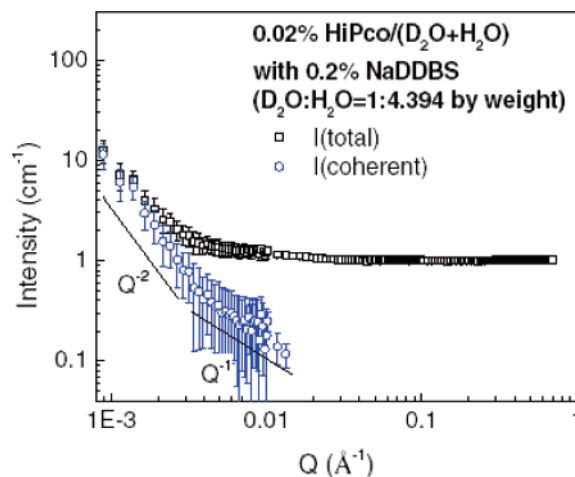
Figure 3. SANS scattering profile from a suspension for which the contrast between surfactant and solvent has been matched by mixing D_2O with H_2O in the ratio 1:4.394 by weight. The concentration of HiPco is 0.02 wt %, and the ratio of nanotube to surfactant is 1:10. After subtracting the incoherent background, the -2 slope at low Q is apparent, and a plausible -1 slope above $Q = 0.003$ Å^{-1} is observed. Reprinted with permission from ref 26. Copyright 2004 Elsevier.

polymer matrices. Given the variability in sizes (both diameter and length), size characterization is best accomplished with an imaging method, specifically atomic force microscopy (AFM).[20,21] If one assumes that the objects on the substrate are representative of the suspension, then a thorough analysis of diameter (inferred from height), length, and aspect ratio is possible.

Second, to what extent do the nanotubes (isolated, ropes, bundles) behave as rigid rods while in suspension? When CNT behave like rigid rods, a variety of rigid-rod theories can be used to explore the physical properties of nanotube suspensions and nanotube/polymer composites.[22-24] This question is readily addressed with scattering methods,[25-29] though some have used rheological[30,31] characterization with success. A limited number of researchers have used small-angle X-ray, neutron, or light scattering with wave vectors Q in the range $10^{-3}-10^0$ nm^{-1} (corresponding to length scales $1-1000$ nm) to investigate nanotubes structures in suspension. A suspension of *isolated* rigid rods with diameter D and length L exhibits scattering intensity that varies as Q^{-1} for wave vectors $2\pi/L < Q < 2\pi/D$. With typical nanotube aspect ratios of >100 and SWNT diameters on the order of ~ 1 nm, the criteria of isolated rigid rods with good dispersion specifies very low nanotube concentration and correspondingly low scattering intensities from nanotube suspensions, wherein lies the challenge. Using small-angle neutron scattering and a dilute suspension of SWNT $(0.01-0.1$ wt %) in water with the surfactant sodium dodecylbenzenesulfonate (NaDDBS), Zhou et al.[26] found the scattered intensity to decrease as Q^{-1} in the range $0.003 < Q < 0.02$ Å^{-1} (Figure 3), consistent with an isolated rigid-rod behavior in these suspensions. In contrast, when the above suspensions were prepared with Triton X-100, a surfactant with less efficient nanotube dispersing ability, the scattered intensity followed a power law dependence with exponents in the range of -2 to -3 over the entire range of Q, suggesting some sort of network of ropes.[26] Wang et al. propose using the exponent of Q as a semiquantitative measure of the degree of dispersion in nanotube suspensions, where exponents closer to -1 indicate better nanotube dispersion.[27] The caveat in these scattering methods is that the observed persistence length that gives rise to the -1 dependence might be small relative to the nanotube length.

Third, how do the nanotube suspensions evolve with time? The stability of nanotube suspensions influences how they can

be handled during processing and in applications. The experimental methods described above to probe size and rigidity can be used to follow nanotube suspensions as a function of time, though few have done so. Overall nanotube dispersions remain an active research area focusing on assessing the size distribution of suspended nanotube objects as well as their rigidity and stability.

4. Nanotube Functionalization

Local strain in carbon nanotubes, which arises from pyramidalization and misalignment of the π-orbitals of the sp²-hybridized carbon atoms, makes nanotubes more reactive than a flat graphene sheet, thereby paving the way to covalently attach chemical species to nanotubes.[32] This covalent functionalization of nanotubes can improve nanotube dispersion in solvents and polymers. For example, SWNT covalently functionalized with pyrrolidine by the 1,3-dipolar cycloaddition of azomethine ylides show a solubility of 50 mg/mL in chloroform, even without sonication whereas the pristine SWNT is completely insoluble in this solvent.[33] Furthermore, covalent functionalization can provide a means for engineering the nanotube/polymer interface for optimal composite properties. With respect to mechanical properties, for example, the interfacial adhesion could be modified through covalent or noncovalent interactions between the functional group on the nanotube and the polymer matrix to maximize load transfer. The open-end functionalization method is widely reported and uses an oxidative route (usually by refluxing in nitric acid) to form shortened nanotubes bearing carboxylic acid end groups that are subsequently converted into other functional groups via standard condensation reactions. Alternatively, various reaction protocols can covalently functionalize primarily the sidewalls of the nanotubes, which is comparatively less destructive to the nanotube length. The reviews by Sung et al.[34] and Dyke et al.[35] give an overview of the current state of the open-end and sidewall covalent functionalization of nanotubes, respectively.

A notable drawback of covalent functionalization is the disruption of the extended π conjugation in nanotubes. While the impact of disrupted π conjugation is limited for mechanical and probably thermal properties, the impact on electrical properties is expected to be profound because each covalent functionalization site scatters electrons. Noncovalent functionalization is an alternate method for tuning the interfacial properties of nanotubes. Star et al.[20,36] achieved such functionalization by adsorbing different polymers onto SWNT to improve the SWNT solubilization. This process has been dubbed "polymer wrapping" of nanotubes, although periodic helical wrapping has only been demonstrated when the polymers are DNA molecules.

5. Nanotube/Polymer Composites

The properties of polymer nanocomposites containing carbon nanotubes depend on several factors in addition to the polymer: synthetic process used to produce nanotubes; nanotube purification process (if any); amount and type of impurities in the nanotubes; diameter, length, and aspect ratio of the nanotube objects in the composite (isolated, ropes, and/or bundles); nanotube orientation in the polymer matrix. These variations in nanotubes and nanotube/polymer composites account for many of the apparent inconsistencies in the literature. Reporting the nanotube concentration (specifying whether the concentration allots for the impurities or functionalization) and the matrix polymer alone is insufficient. Although the variations listed above are difficult to quantify, more complete reporting will

reduce the discrepancies between the published results of similar composites. Researchers might also adapt the protocol used in our lab in which entire studies are performed using nanotubes materials from the same batch of purified nanotubes, thereby reducing the variability between samples and clarifying trends.

The next two sections present various fabrication techniques targeting good nanotube dispersion and nanotube alignment. Subsequent sections highlight the mechanical, electrical, rheological, thermal, and flammability properties of nanotube/polymer composites.

5.1. Fabrication of Nanotube/Polymer Composites. Fabrication methods have overwhelmingly focused on improving nanotube dispersion because better nanotube dispersion in the polymer matrices has been found to improve properties. Similar to the case of nanotube/solvent suspensions, pristine nanotubes have not yet been shown to be soluble in polymers illustrating the extreme difficulty of overcoming the inherent thermodynamic drive of nanotubes to bundle. The quality of nanotube dispersion in polymer matrices should be evaluated over a range of length scales and can be accomplished using a selection of these imaging methods: optical microscopy, polarized Raman imaging,[37] scanning electron microscopy (SEM), and transmission electron microscopy (TEM). More recently, confocal microscopy has been successfully applied to evaluate the nanotube dispersion in MWNT/polystyrene nanocomposites.[38] Scattering methods remain difficult to interpret regarding dispersion in polymers because the contrast is low and the presence of rigid-rod behavior ($I \propto Q^{-1}$) is not equivalent to good dispersion at all length scales. At a local length scale, UV−vis−near-IR spectroscopy qualitatively determines the nanotube dispersion state in SWNT solutions and nanocomposites because only individual or small bundles of SWNT exhibit sharp absorbance peaks (van Hove singularities), while large bundles exhibit only monotonically decreasing absorbance with increasing wavelength.[39]

The methods of solution blending, melt blending, and in situ polymerization are widely applied to produce nanotube/polymer composites and will be summarized here. In addition, latex technology, solid-state shear pulverization, and coagulation spinning methods also show promise.

Solution Blending. This is the most common method for fabricating polymer nanocomposites because it is both amenable to small sample sizes and effective. Solution blending involves three major steps: disperse nanotubes in a suitable solvent, mix with the polymer (at room temperature or elevated temperature), and recover the composite by precipitating or casting a film. As mentioned earlier, it is difficult to disperse the pristine nanotubes, especially SWNT, in a solvent by simple stirring. High-power ultrasonication can be used to make metastable suspensions of nanotubes or nanotube/polymer mixtures in different solvents. Note that high-power ultrasonication for a long period of time shortens the nanotube length, i.e., reduces the aspect ratio, which is detrimental to the composite properties.[24] The minimum sonication conditions (time, power) that produce CNT degradation are yet to be determined and will certainly depend on nanotube concentration and initial nanotube length distribution.

One variation of the solution blending method uses surfactants to disperse higher loadings of nanotubes.[21,40,41] Islam et al.[21] dispersed SWNT (20 mg/mL) in water with the aid of the surfactant NaDDBS (NaDDBS:SWNT = 1:10) using low-power, high-frequency (12 W, 55 kHz) sonication for 16−24 h. Atomic force microscopy revealed that ∼63 ± 5% of SWNT bundles are exfoliated into single tubes. While the majority of

SWNT objects are isolated SWNT, the isolated SWNT account for less than a quarter of the SWNT by mass. Using surfactants to improve nanotube dispersion can be problematic because the surfactant remains in the resulting nanocomposite and might degrade transport properties. For example, Bryning et al.[41] reported that the thermal conductivities of the surfactant-SWNT/ epoxy composites are much lower (and the interfacial thermal resistances are higher) than that of the composites prepared without surfactant at the same loading. The surfactant molecules can also alter the polymer matrix as shown by Sundararajan et al.,[42] where Triton X-100 induced crystallization in polycarbonate (PC); crystallization might in turn affect the transparency and mechanical properties of the composites. One alternative to surfactant-aided dispersion is nanotube functionalization to improve dispersion and interfacial adhesion to the polymer matrix; examples of functionalization appear later.

When using solution blending, nanotubes tend to agglomerate during slow solvent evaporation, leading to inhomogeneous distribution of the nanotubes in the polymer matrix. The evaporation time can be reduced by putting the nanotube/ polymer suspension on a rotating substrate (spin-casting[43]) or dropping the nanotube/polymer suspension on a hot substrate (drop-casting[44]). Singh et al.[45] developed a wet annealing method that produces transparent films of polycarbonate containing 0.06−0.25 wt % SWNT. Their wet annealing method involves partially drying a nanotube/polymer suspension on a substrate and then increasing the temperature ($T > T_g$) to rapidly complete the drying process. SEM images of the fracture surface of the films showed a long-range, entangled network of SWNT even at 0.06 wt % nanotube loading. To avoid agglomeration during solvent evaporation, Du et al.[46] developed the versatile coagulation method that involves pouring a nanotube/polymer suspension into an excess of nonsolvent. The precipitating polymer chains entrap the SWNT, thereby preventing the SWNT from bundling. When this coagulation method is applied to poly-(methyl methacrylate) (PMMA), optical microscopy, SEM, and Raman imaging indicate good dispersion of SWNT in the nanocomposite. This method has been adapted to polyethylene (PE), where the nanotube/polymer suspension is heated to promote polymer solubility and then cooled to accomplish the precipitation.[47]

Melt Blending. Melt blending uses high temperature and high shear forces to disperse nanotubes in a polymer matrix and is most compatible with current industrial practices. However, relative to solution blending methods, melt blending is generally less effective at dispersing nanotubes in polymers and is limited to lower concentrations due to the high viscosities of the composites at higher nanotube loadings. Successful examples of melt blending include MWNT/polycarbonate,[48] MWNT/ nylon-6,[49,50] SWNT/polypropylene,[51] and SWNT/polyimide[52] composites. Haggenmueller et al.[53] combined solution and melt blending by subjecting a solvent cast SWNT/polymer film to several cycles of melt pressing. An approach developed by Jin et al.[54] introduces polymer-coated MWNT (rather than pristine MWNT) into the polymer melt to promote compatibilization.

In Situ Polymerization. This fabrication strategy starts by dispersing nanotubes in monomer followed by polymerizing the monomers. As with solution blending, functionalized nanotubes can improve the initial dispersion of the nanotubes in the liquid (monomer, solvent) and consequently in the composites. Furthermore, in situ polymerization methods enable covalent bonding between functionalized nanotubes and the polymer matrix using various condensation reactions. Epoxy nanocomposites comprise the majority of reports using in situ polym-

erization methods,[41,55−60] where the nanotubes are first dispersed in the resin followed by curing the resin with the hardener. Zhu et al.[56] prepared epoxy nanocomposites by this technique using end-cap carboxylated SWNT and an esterification reaction to produce a composite with improved tensile modulus (E is 30% higher with 1 wt % SWNT). Note that as polymerization progresses and the viscosity of the reaction medium increases, the extent of in situ polymerization reactions might be limited. Noteworthy extensions of in situ polymerization include infiltration methods in which the reactive agents are introduced into a nanotube structure and subsequently polymerized.[61−64]

Other Methods. Rather than avoid the high viscosities of nanotube/polymer composites, some researchers have decreased the temperature to increase viscosity to the point of processing in the solid state. Solid-state mechanochemical pulverization processes (using pan milling[65] or twin-screw pulverization[66]) have mixed MWNT with polymer matrices. Pulverization methods can be used alone or followed by melt mixing. Nanocomposites prepared in this manner have the advantage of possibly grafting the polymer on the nanotubes, which account in part for the observed good dispersion, improved interfacial adhesion,[65] and improved tensile modulus.[65,66]

An innovative latex fabrication method for making nanotube/ polymer composites disperses nanotubes in water (SWNT require a surfactant, MWNT do not) and then adds a suspension of latex nanoparticles.[67,68] Freeze-drying and subsequent processing of this colloidal mixture produces composites with uniform dispersion of nanotubes even in a highly viscous matrix like high molecular weight polystyrene.[67] This promising method can be applied to polymers that can be synthesized by emulsion polymerization or formed into artificial latexes, e.g., by applying high-shear conditions.

Finally, to obtain nanotube/polymer composites with very high nanotube loadings, Vigolo et al.[69] developed a "coagulation spinning" method to produce composite fibers comprising predominately nanotubes. This method disperses SWNT using a surfactant solution, coagulates the nanotubes into a mesh by wet spinning it into an aqueous poly(vinyl alcohol) solution, and converts the mesh into a solid fiber by a slow draw process. In addition, Mamedov et al.[70] developed a fabrication method based on sequential layering of chemically modified nanotubes and polyelectrolytes to reduce phase separation and prepared composites with SWNT loading as high as 50 wt %.

5.2. Alignment of Nanotubes in the Composites. The high aspect ratios of nanotubes make them susceptible to orientation either intentionally via various fiber spinning methods or unintentionally via solvent casting, filtering, or melt pressing. Small-angle and wide-angle X-ray scattering as well as polarized Raman spectroscopy can quantify the degree of alignment in the composites. When investigating properties, researchers must consider the possibility of nanotube orientation and how the presence of nanotube alignment could alter their conclusions.

Nanotube alignment can be achieved prior to composite fabrication where aligned nanotubes are incorporated into a polymer matrix by in situ polymerization. Raravikar et al.[61] and Feng et al.[62] prepared aligned nanotube composites of PMMA and polyaniline, respectively, by infiltrating monomers into CVD-grown arrays of aligned MWNT, followed by in situ polymerization with no observable degradation of the MWNT alignment.[61] Alternatively, in situ polymerization can be performed in the presence of an external field (e.g., a magnetic field[71]), where viscosity of the nanotube−monomer suspension affects the degree of alignment.
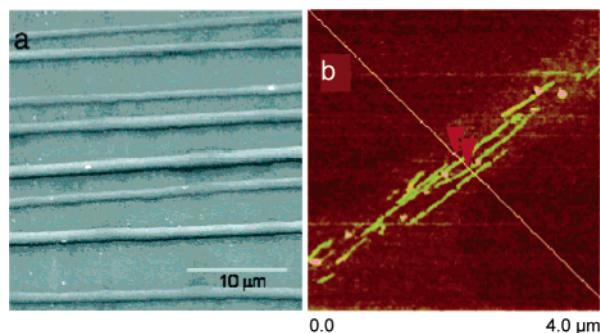
Figure 4. (a) SEM image of aligned electrospun fibers. (b) AFM image of aligned individual SWNT after heating an electrospun fiber on a silicon substrate. From ref 76.

The nanotubes can also be aligned during or after the composite fabrication by mechanical stretching,[72] spin-casting,[73] wet spinning, melt fiber spinning,[53,74] and electrospinning,[75−78] where the last two methods offer the greatest degree of alignment. In melt fiber spinning, the composite melt is extruded through a spinneret hole, and the extruded rod is air cooled and drawn under tension by a windup spool to produce aligned composite fibers. Haggenmueller et al.[74] found that the degree of alignment increases with decreasing fiber diameter (due to greater extensional flow) and decreases with increasing nanotube loading (due to agglomeration and restrictions in motion from neighboring nanotubes). Electrospinning produces composite nanofibers using electrostatic forces as demonstrated by Gao et al.[76] in SWNT/poly(vinyl pyrrolidone) fibers (Figure 4a). The SWNT exhibit good alignment and dispersion, as characterized by AFM after the removal of the polymer matrix by heating.

The physical properties of nanotube/polymer composites, which we discuss next, arise from the nanotube and polymer characteristics as well as from the microstructures produced while fabricating and processing these nanocomposites. Thus, ongoing efforts must improve our morphological control in nanotube/polymer composites using a combination of practicality and creativity. Note that the optimal microstructure for one physical property might not be the best microstructure of another physical property. Developing robust correlations (if not quantitative predictions) between nanotube/polymer composites and their properties will further advance the design and engineering of these composites.

6. Mechanical Properties

The fiberlike structure of carbon nanotubes, their low density, high aspect ratio, and extraordinary mechanical properties make them particularly attractive for reinforcement in composite materials. The outstanding potential of carbon nanotubes as reinforcements in polymer composites is evident from the super-tough composite fibers fabricated by Dalton et al.[79] By optimizing the "coagulation spinning" method,[69] they spun several hundred meters of composite fibers of 60 wt % SWNT/poly-(vinyl alcohol), which had a tensile strength of 1.8 GPa, comparable to that of a spider silk. Using these fibers, they were able to make 100 μm diameter supercapacitors and electronic textiles. To take advantage of the inherent properties of polymers (e.g., transparency and flexibility), it is often desirable to use a low concentration of fillers in the composites, much lower than the 60 wt % employed by Dalton et al.[79]

In general, the tensile modulus and strength of polymer-rich nanotube composites are found to increase with nanotube loading, dispersion, and alignment in the matrix. However, the results at low nanotube concentrations typically remain far behind the idealized theoretical predictions from the rule of mixtures[80] and the Halpin−Tsai model.[81] For example, Haggenmueller et al. found that the tensile modulus of PE fiber was improved from 0.65 to 1.25 GPa with the addition of 5 wt % SWNT (aspect ratio ∼380).[74] The Halpin−Tsai model would predict the modulus to be ∼16 GPa at this nanotube loading (assuming the modulus of SWNT is 1000 GPa). At higher nanotube loadings, the extent of improvement in mechanical properties might be limited by the high viscosity of the composite and the resulting void defects.[57]

The gap between the predictions and experimental results arises from imperfect dispersion and poor load transfer. Even modest nanotube agglomeration impacts the diameter and length distributions of the filler and overall is likely to decrease the aspect ratio (a parameter in the models). In addition, nanotube agglomeration reduces the modulus of the filler (another parameter in the models) relative to that of isolated nanotubes because there are only weak dispersive forces between nanotubes. Schadler et al.[55] and Ajayan et al.[59] concluded from Raman spectra that slippage occurs between the shells of multiwall nanotubes and within single-wall nanotube ropes and may limit stress transfer in nanotube/polymer composites. While the load transfer at the nanotube/polymer interface is certainly less than ideal, there are several reports of strong interactions. For example, Wagner et al.[82] found that the average interfacial stress required to remove a single MWNT from the polyethylene−butene matrix is 47 MPa, which is about 10 times larger than the adhesion level between the same type of polymer and carbon fibers; this example demonstrates the importance of filler size on the interfacial strength. It is important to understand the mechanism of interfacial adhesion at the molecular level to further optimize the interface in nanocomposite systems. Using molecular mechanics simulations and elasticity calculations, Liao et al.[83] found that in the absence of atomic bonding between the nanotubes and the matrix the nanotube/matrix adhesion comes from (i) electrostatic and van der Waals interactions and (ii) stress/deformation arising from the mismatch in the coefficients of thermal expansion between nanotubes and the polymer matrix. Several other mechanisms[84] have been proposed to describe these interfaces, and further investigations are necessary to understand and then optimize nanotube/polymer interfaces.

Functional moieties on nanotubes typically provide better interfacial load transfer via bonding and/or entanglement with the polymer matrix. Molecular simulation by Frankland et al.[85] predicted that chemical bonding between SWNT and the polymer matrix with only ∼0.3% grafting density can increase the shear strength of a polymer−nanotube interface by over an order of magnitude. Experimentally, Geng et al.[86] obtained a 145% increase in tensile modulus and 300% increase in yield strength with 1 wt % fluorinated SWNT in a poly(ethylene oxide) matrix. In situ ring-opening polymerization of caprolactam by Gao et al.[87] in the presence of carboxylated SWNT produced SWNT/nylon-6 composites with nylon chains grafted to the SWNT. The stress−strain profile of these composite fibers indicate a 153% increase in Young's modulus and 103% increase in tensile strength with 1 wt % carboxylated SWNT (Figure 5). In fact, at low SWNT loadings (<0.5 wt %) the experimental Young's moduli of these composite fibers approximate the Halpin−Tsai predictions for an aligned composites, and the tensile strength is higher than the theoretical rule of mixture estimate. This suggests that the covalent bonding at the nanotube/polymer interface can be very effective in strengthening the material.
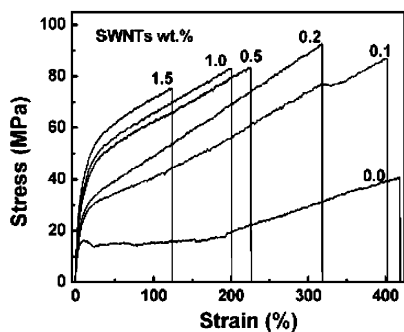
Figure 5. Stress−strain profiles of SWNT−nylon-6 composite fibers at different SWNT loadings. The curves are labeled with the percentage of SWNT in the polymer matrix. From ref 87.
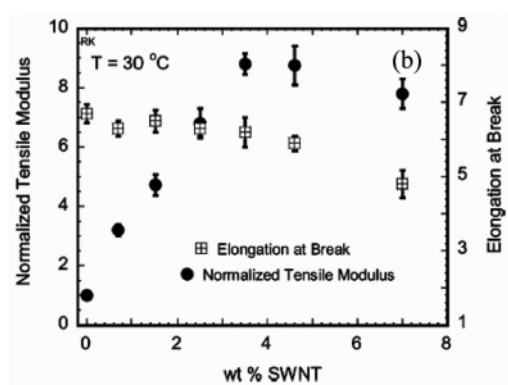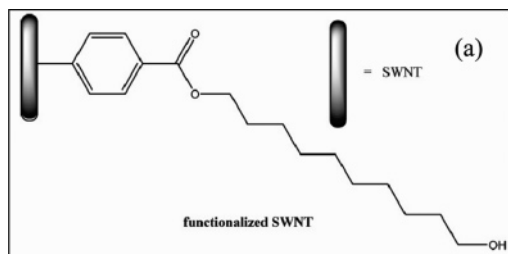

Figure 6. (a) Structure of the functionalized SWNT used for the fabrication of PDMS nanocomposite (SWNT not drawn to scale). (b) Composition dependence of the normalized tensile modulus ($E_{composite}/E_{PDMS}$) and the elongation at break ($L_{break}/L_{initial}$) for SWNT/PDMS nanocomposites. From ref 17.

Note that the improvements in tensile strength and modulus in Figure 5 are coupled with a reduction in strain at break, indicating a decrease in polymer toughness and flexibility. This is a common phenomenon even in commercial composites but might be particularly problematic while trying to modify elastomers for applications such as tires, belts, seals, O-rings, etc. A promising result from Dyke et al.[17] reports the fabrication of poly(dimethylsiloxane) (PDMS) composites with functionalized SWNT, where they found that the tensile modulus and strength are considerably increased in these composites whereas the strain at break is largely unchanged (Figure 6). The functional groups on the nanotube sidewalls were designed to improve the compatibility with the polymer matrix. Their fabrication strategy can be readily extended to a wide range of elastomers and network-forming polymers.

7. Electrical Conductivity

The potential of nanotubes as conducting fillers in multifunctional polymer composites has been successfully realized. Several orders of magnitude enhancement in electrical conductivity (σ) has been achieved with a very small loading (0.1 wt
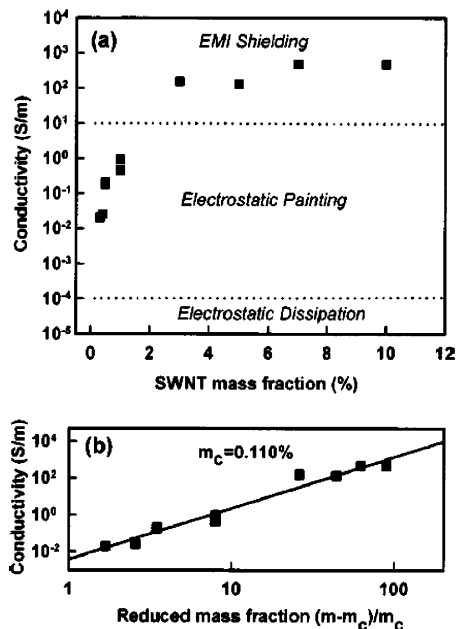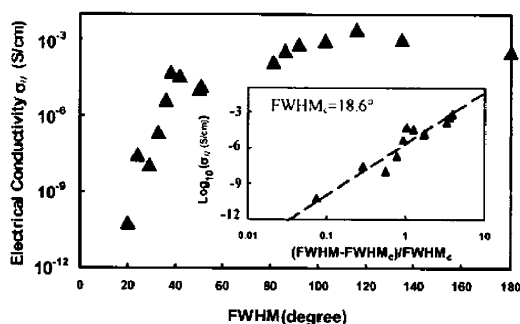

Figure 7. (a) Electrical conductivity of SWNT/polycarbonate nanocomposites as a function of nanotube loading, showing a typical percolation behavior. Dashed lines represent the lower limits of electrical conductivity required for the specified applications. (b) Electrical conductivity as a function of reduced mass fraction of nanotubes, showing a threshold of 0.11 wt %. Reprinted with permission from ref 89. Copyright 2003 American Institute of Physics.

% or less[22]) of nanotubes in the polymer matrices, while maintaining the other performance aspects of the polymers such as optical clarity, mechanical properties, low melt flow viscosities, etc. A variety of applications are being pursued using these conductive composites: electrostatic dissipation, electrostatic painting, electromagnetic interference (EMI) shielding, printable circuit wiring, and transparent conductive coating.[88] Figure 7a shows the electrical conductivity of SWNT/polycarbonate (PC) composites as a function of nanotube loading;[89] compositions >0.3 wt % and >3 wt % SWNT loading are sufficient for applications in electrostatic painting and EMI shielding, respectively, in these solution-blended composites.

Composites containing conducting fillers in insulating polymers become electrically conductive when the filler content exceeds a critical value, known as a percolation threshold. The percolation threshold is characterized by a sharp jump in the conductivity by many orders of magnitude which is attributed to the formation of a three-dimensional conductive network of the fillers within the matrix. The percolation threshold is typically determined by plotting the electrical conductivity as a function of the reduced mass fraction of nanotubes and fitting with a power law function (Figure 7b). The nanotube/polymer composites exhibit very low percolation threshold for electrical conductivity because of the large aspect ratio and the nanoscale dimension of nanotubes. For SWNT/polymer composites, the reported percolation thresholds range from 0.005 vol % to several vol %.[22] Percolation thresholds as low as 0.002 vol % have been achieved in the polymer composite with long flexible ropes of aligned MWNT.[90]

The percolation threshold for the electrical conductivity in nanotube/polymer composites is influenced by several nanotube characteristics: aspect ratio,[22,91] dispersion,[40] and alignment.[23,46,53] Bryning et al.[22] prepared SWNT/epoxy composites with nanotubes from two different sources, HiPco and laser oven, having aspect ratios of ∼150 and ∼380, respectively, and found a smaller percolation threshold with the higher aspect

Figure 8. Electrical conductivity of a 2 wt % SWNT/PMMA composite along the alignment direction with increasing nanotube isotropy. Nanotube alignment is assessed using X-ray scattering where fwhm = 0 is perfectly aligned and fwhm = 180 is isotropic. Inset: a log−log plot of electrical conductivity vs reduced fwhm determines the critical alignment, fwhm$_c$. Reprinted with permission from ref 23. Copyright 2005 American Physical Society.

ratio nanotubes. Bai and Allaoui[91] found more than an 8-fold decrease in the threshold concentration in MWNT/epoxy composites when the MWNT length was increased from 1 to 50 μm. Well-dispersed nanotubes generally have higher aspect ratios than nanotube aggregates, so the percolation threshold decreases with better dispersion. Counter examples include work by Bryning et al.[22] and Martin et al.[92] where slight aggregation produces a lower percolation threshold by increasing the local interactions between nanotubes. Alignment of the nanotubes in the polymer matrix has a profound effect on the electrical conductivity and its percolation threshold. When the nanotubes are highly aligned in the composites, there are fewer contacts between the tubes, which results in a reduction in electrical conductivity and a higher percolation threshold as compared to those in a composite with randomly oriented nanotubes. This topic has been extensively studied by Du et al.[23] using a series of SWNT/PMMA composites where the degree of nanotube alignment was controlled by the melt fiber spinning conditions and quantified with the full width at half-maximum (fwhm) of the SWNT form factor scattering, where higher fwhm correspond to less SWNT alignment. At a fixed SWNT concentration (2 wt %), the electrical conductivity parallel to the alignment direction increased sharply with decreasing alignment (Figure 8), which they term orientation percolation. Figure 8 also indicates that there are intermediate levels of nanotube alignment (fwhm ∼ 100°−140°) where the electrical conductivities are higher than the isotropic condition (fwhm 180°). These experimental findings were cohobated using a simple 2D Monte Carlo simulation.[23]

It is widely accepted that chemical functionalization disrupts the extended π-conjugation of nanotubes and thereby reduces the electrical conductivity of isolated nanotubes. However, we note that several researchers[93−96] report that functionalization can improve the electrical properties of the composites. For example, Valentini et al.[96] pointed out that the amine-functionalized SWNT in epoxy matrix allows migration of intrinsic charges, which contribute to the overall conductivity. Tamburri et al.[95] found that extensive functionalization of SWNT with −OH and −COOH groups enhances the current in a conducting polymer (1,8-diaminophthalene) by factors of 90 and 140, respectively, whereas the untreated tubes showed an enhancement of only 20. It appears that the disadvantages of functionalization with respect to SWNT conductivity are outweighed by the improved dispersion enabled by functionalization.
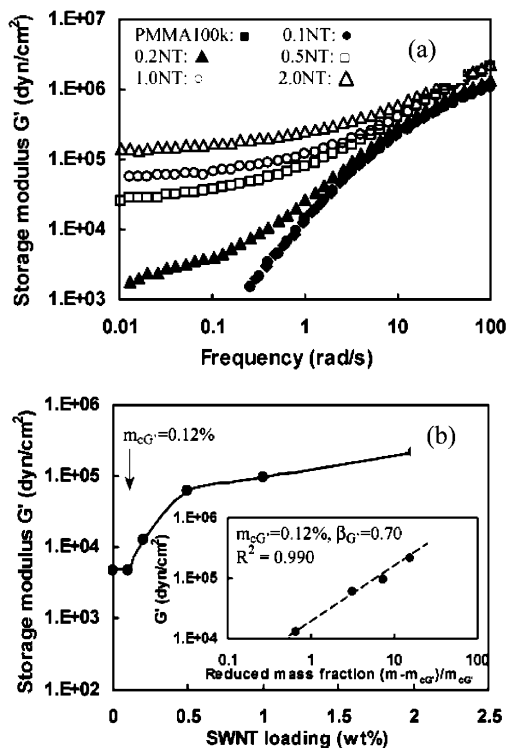
Figure 9. (a) Storage modulus (G') vs shear frequency for SWNT/PMMA nanocomposites with various nanotube loadings from 0 to 2.0 wt %. (b) G' as a function of the nanotube loading for SWNT/PMMA nanocomposites at a fixed frequency, 0.5 rad/s. Inset: a power law plot of G' vs reduced mass fraction on a logarithmic scale. From ref 37.

8. Rheological Properties

The viscoelastic properties of nanotube/polymer composites have both practical importance related to composite processing and scientific importance as a probe of the composite dynamics and microstructure. Figure 9 shows the storage modulus (G') as a function of frequency for a typical response of nanotube/polymer composites with good nanotube dispersion.[37] At high frequencies, the response is not sensitive to the filler concentration, indicating that the short-range polymer dynamics are not influenced by the nanotubes. In a consistent manner the glass transition temperatures of the composites are constant in the absence of strong interfacial bonds and at low nanotube loadings. At low frequencies, the rheological behavior progresses from a liquidlike response ($G' \propto \omega^{-2}$) to a solidlike response (G' independent of ω) as the nanotube concentration increases. This is consistent with earlier findings in silicate nanocomposites.[97] Applying a power law function to the G' vs nanotube loading data provides a rheological percolation threshold ($m_{cG'}$) corresponding to the onset of solidlike behavior (Figure 9b).

As with electrical percolation, the rheological percolation is found to depend on nanotube dispersion, aspect ratio, and alignment. Mitchell et al.[98] improved dispersion by functionalizing SWNT such that the rheological percolation threshold dropped from 3 wt % when using pristine SWNT to 1.5 wt % in functionalized SWNT/polystyrene composites. The values of G' at low frequencies were also higher for the functionalized composites, indicating better load transfer between the nanotube network and the polymer. The effect of aspect ratio (shape) was illustrated by comparing nanotube and layered silicate nanofillers, which are disk-shaped and require a higher loading to form a percolated network.[99] Within a given system (nanotubes and polymers), the linear viscoelastic response can serve as an

indirect qualitative measure of the dispersion state of the nanotubes in the composites, where better dispersion corresponds to higher value of G' or a lower slope.

Potschke et al.[100] also found that the rheological percolation threshold is strongly dependent on temperature. In their SWNT/PC composite, the percolation threshold decreases from ~5 to 0.5 wt % MWNT upon increasing T from 170 to 280 °C. They suggest that the superposition of the entangled polymer network and the combined nanotube−polymer network rather than the nanotube network alone dominates the rheological properties. The concentration of nanotubes required to form a reinforcing nanotube−polymer network should be lower than the electrical percolation threshold, which requires nanotube−nanotube contacts to form a conductive network. In fact, in a set of SWNT/PMMA composites, Du et al.[37] found that the rheological percolation threshold, 0.12 wt %, was significantly smaller than the percolation threshold for electrical conductivity, 0.39%. In contrast, the nanotube−nanotube network appears to dominate the rheological response of nanotube suspensions.[101]

9. Thermal Conductivity

The thermal conductivity, κ, of carbon materials is dominated by atomic vibrations or phonons. Nanocomposites with good thermal conductivity have potential applications in printed circuit boards, connectors, thermal interface materials, heat sinks, and other high-performance thermal management systems. The excellent thermal conductivity of individual nanotubes led to early expectations that it will enhance the thermal conductivity of polymer nanocomposites, as nanotubes do with the electrical conductivity. In contrast to the orders of magnitude enhancement in electrical conductivity with very low loading of nanotubes (less than 0.1 wt %) (see Figures 7 and 8), the thermal conductivities of the composites have shown only modest improvement. Note, however, that the highest reported nanotube thermal conductivities are on the order of 10^3 W/(m K), while typical thermoplastics have $\kappa \sim 0.1$ W/(m K). (Note that the thermal conductivity of isolated nanotubes is an active area of research with some reports giving values as low at 30 W/mK; see work by Zhong et al.[102]) Thus, phonons entering a nanotube/polymer composite are much more likely to travel through the matrix than electrons because the contrast in thermal conductivity ($\kappa_{nanotube}/\kappa_{polymer}$) is ~$10^4$ in comparison to the electrical conductivity contrast ($\sigma_{nanotube}/\sigma_{polymer}$) of ~$10^{15}$–$10^{19}$. In addition to the lack of thermal conductivity contrast, the design of nanotube/polymer composites with high thermal conductivity must also address the high interfacial thermal resistance between nanotubes (more on this below). The composite thermal conductivity will (of course) also depend on the attributes discussed previously (aspect ratio, dispersion, alignment) and might be more sensitive to metal impurities.

Here we summarize the more promising experimental findings. Biercuk et al.[103] prepared an epoxy composite with 1 wt % raw (not purified) laser-oven SWNT that showed a 125% increase in thermal conductivity at room temperature. Choi et al.[104] reported a 300% increase in thermal conductivity at room temperature with 3 wt % SWNT in epoxy, with an additional increase (10%) when aligned magnetically. Du et al.[63] developed an infiltration method that produces a bicontinuous morphology of epoxy and a nanotube-rich phase and shows a ~220% increase in thermal conductivity at ~2.3 wt % SWNT loading. This two-phase material with very poor dispersion at the nanoscale demonstrates an approach that circumvents the need for good dispersion to produce favorable properties.

The improvements in thermal conductivity cited above are all well below the prediction of the engineering rule of mixing.

Huxtable et al.[105] attributed this discrepancy to the exceptionally small thermal conductance ($G \approx 12$ MW/(m^2 K)) of the nanotube−polymer interface, i.e., high interfacial thermal resistance. This interfacial thermal resistance arises from the constraints that the energy contained in high-frequency phonon modes within the nanotubes must first be transferred to low-frequency modes through phonon−phonon coupling in order to be exchanged with the surrounding medium. Simulations of heat transfer between two nanotubes without an intervening matrix material also show high thermal resistance.[105] This result is consistent with the low thermal conductivity of SWNT films or so-called buckypapers (~30 W/(m K) for the unaligned buckypaper[106]) as compared to that of the individual SWNT-(~6600 W/(m K), theoretical prediction[8]). From a comparative study of different nanotubes (SWNT, MWNT, DWNT) in epoxy composites, Gojny et al. suggest that MWNT have the highest potential to improve the thermal conductivity of polymer composites because of their relatively low interfacial area (therefore, less phonon scattering at the interface) and the existence of shielded internal layers which promote the conduction of phonons and minimizes the matrix coupling losses.[107]

One approach to reducing the high thermal interfacial resistance is the introduction of covalent bonds between nanotubes and the matrix polymer. Shengoin et al.[108] found a significant reduction in the tube−matrix thermal boundary resistance in the presence of chemical bonding using classical molecular dynamics. Unfortunately, such bonds decrease the intrinsic tube conductivity by acting as scattering centers for phonons propagating along the tubes. In a simulation of (10,-10) SWNT, they observed that the composite thermal conductivity improves with functionalization only if the tubes have aspect ratios of 100 to 1000; at larger aspect ratios, composites with unfunctionalized tubes are better. Experimental work by Liu et al.[109] using 2 wt % carboxylic acid functionalized MWNT in PDMS found that chemical functionalization degrades thermal conductivity more severely than predicted by Shengoin et al.[108]

A recent report by Huang et al.[64] is thus far the most promising result on thermal conductivity enhancement by nanotubes in polymer composites. Starting with an aligned CVD grown MWNT arrays (0.05−0.5 mm high, Figure 10a), they embedded the array with silicone elastomers using an injection molding method. The MWNT span the composite film with all the nanotube tips revealed on both surfaces; the protruding tips ensured better thermal contact with the heat source. The thermal conductivity of such a composite containing 0.4 vol % (0.3 wt %) aligned MWNT is ~115−280% higher than either the pure polymer or a composite with 0.4 vol % of dispersed MWNT (Figure 10b). Future work is likely to improve upon these results because this preparation method could incorporate as high as 10 vol % nanotube to deliver a thermal conductivity perhaps an order of magnitude higher than typical current commercial thermal interface materials.

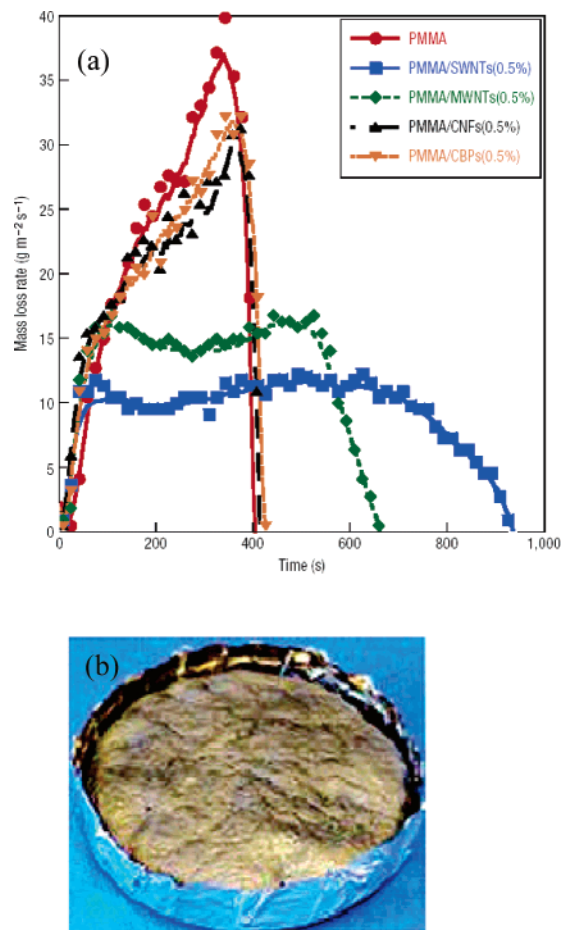### 10. Thermal Stability and Flammability

Using thermogravimetric analysis (TGA), several groups have reported improved thermal stability in nanotube/polymer composites relative to the polymers. Specifically, the onset decomposition temperature, T_{onset}, and the temperature of maximum weight loss rate, T_{peak}, are higher in the nanocomposites. For example, Ge et al.[75] found that 5 wt % MWNT/PAN composite fibers showed a 24° C shift in T_{onset} as compared to that of the neat PAN. A number of mechanisms have been suggested. Dispersed nanotubes might hinder the flux of degradation product and thereby delay the onset of degradation. Polymers
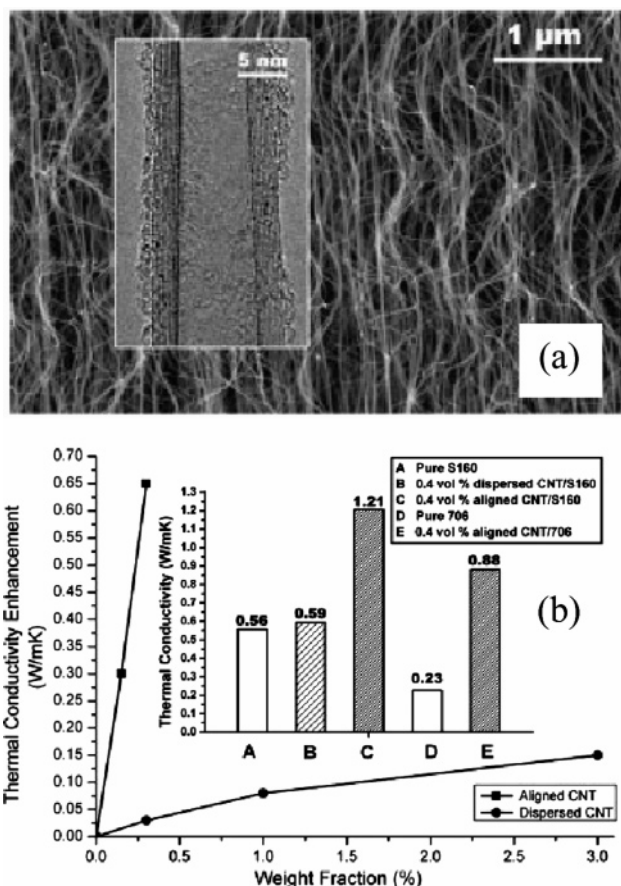
Figure 10. (a) SEM image of the side view of an aligned MWNT array. Inset: a high-resolution TEM image of an isolated MWNT showing eight nested nanotubes. (b) Thermal conductivity enhancement ($\kappa_{composite} - \kappa_{matrix}$) vs weight fraction of MWNT in both aligned and unaligned nanocomposites. Inset: thermal conductivity for selected MWNT/silicone elastomer composites. Reprinted with permission from ref 64. Copyright 2005 Wiley-VCH.

Figure 11. (a) Effect of various nanofillers on mass loss rate when PMMA composites are subjected to an external radiant flux of 50 kW m^{-2} in nitrogen. (b) Residue from the 0.5 wt % SWNT/PMMA composite after the gasification test showing a free-standing nanotube structure. Reprinted with permission from ref 111.

near the nanotubes might degrade more slowly, which would shift T_{peak} to higher temperatures. Another possible mechanism attributes the improved thermal stability to the effect of higher thermal conductivity in the nanotube/polymer composites that facilitates heat dissipation within the composite.[105]

The observed improvement in thermal stability hints that nanotubes could be efficient as fire-retardant additives in polymer matrices. Using a cone calorimeter to evaluate melt-blended composites of 2.5 wt % MWNT/ethylene−vinyl acetate (EVA), Beyer[110] found that MWNT significantly reduces the heat release rate compared with the virgin EVA. In addition, the author found that blends of MWNT and organoclays act as synergistic flame-retardant fillers in the polymer matrix. Kashi-wagi et al.[111,112] found that SWNT act even better as flame-retardant fillers. They compared[111] the flame-retardant abilities of 0.5 wt % SWNT, MWNT, CNF, and carbon black particles in PMMA matrix (Figure 11a). Using a nitrogen gasification test (no flaming but sample heating similar to fire condition), they found that SWNT has the highest capability to reduce the mass loss rate of the composite; MWNT is the second most effective. They attribute the improved flame resistance to the formation of a protective, free-standing nanotube structure that acts a heat shield for the remaining composite below (Figure 11b). This nanotube structure originates in the nanocomposites as the previously discussed nanotube network detected by linear viscoelastic measurements. Consistent with this mechanism, the flame retardancy is found to improve with better dispersion,

higher loading, and higher interface area (aspect ratio) of the nanotubes.[112]

11. Conclusions

In this review, we provide an overview of the research in nanotube/polymer composites and insights to the factors that will ultimately control their properties. In the interest of brevity this is not a comprehensive review. In particular, this review does not attempt to review the patent literature because due to the proprietary nature of patents, it is difficult to get complete information. Given that much of the research on nanotube/polymer composites is application driven and patents are an integral part of this research arena, the omission of patents is notable. The following points are evident about nanotube/polymer composites:

(1) The properties of nanotube/polymer composites depend on a multitude of factors that include the type (SWNT, DWNT, MWNT), chirality, purity, defect density, and dimensions (length and diameter) of the nanotubes, nanotube loading, dispersion state and alignment of nanotubes in the polymer matrix, and the interfacial adhesion between the nanotube and the polymer matrix. These factors should be taken into account when reporting, interpreting, and comparing results from nanotube/polymer composites.

(2) Functionalization of nanotubes provides a convenient route to improve dispersion and modify interfacial properties that may in turn improve the properties of nanocomposites, especially

mechanical properties. The significant progress in nanotube functionalization chemistry in recent years ensures that this approach will become more prevalent.[113,114]

(3) Quantifying nanotube dispersion in polymers (and solvents) is an inherently challenging problem because it involves a range of length scales, and thereby multiple experimental methods are required. Fortunately, new experimental methods are applied to the problem, such as a fluorescence method to nondestructively detect isolated SWNT in a polymer matrix.[115]

(4) Nanotubes have clearly demonstrated their capability as conductive fillers in polymer nanocomposites. Further advances with respect to electrical conductivity in nanotube/polymer composites are likely if only (or predominately) metallic nanotubes could be used in the nanocomposites. Two approaches are actively being pursued in SWNT materials: modify the synthetic route to preferentially produce metallic nanotubes and sort the existing nanotubes.[116]

(5) The physical properties of nanotube/polymer composites can be interpreted in terms of nanotube networks, which are readily detected by electrical and rheological property measurements. The nanotube network provides electrical conduction pathways above the percolation threshold, where the percolation threshold depends on both concentration and nanotube alignment. The nanotube network also significantly increases the viscosity of the polymer and slows thermal degradation. In contrast, it remains a challenge to reduce the interfacial thermal resistance of these nanotube networks, so as to take advantage of the high thermal conductivity of individual nanotubes in a polymer composite system.

In conclusion, nanotube/polymer composites offer both great potential and great challenges, marking it as a vibrant area of work for years to come. The improvement and application of these composites will depend on how effectively we can handle the challenges. The significant progress in the understanding of these composite systems within the past few years points toward a bright future. Finally, one might ask what the next fillers will be for polymers, and the answer might well be more high aspect ratio, nanoscale fillers, such as nanorods and nanowires.[117]

References and Notes

(1) Iijima, S. *Nature (London)* **1991**, *354*, 56−8.

(2) Ajayan, P. M.; Stephan, O.; Colliex, C.; Trauth, D. *Science* **1994**, *265*, 1212−14.

(3) Cooper, C. A.; Young, R. J.; Halsall, M. *Composites, Part A* **2001**, *32A*, 401−411.

(4) Gao, G.; Cagin, T.; Goddard, W. A., III. *Nanotechnology* **1998**, *9*, 184−191.

(5) Uchida, T.; Kumar, S. *J. Appl. Polym. Sci.* **2005**, *98*, 985−989.

(6) De Heer Walt, A. *MRS Bull.* **2004**, *29*, 281−285.

(7) McEuen, P. L.; Bockrath, M.; Cobden, D. H.; Yoon, Y.-G.; Louie, S. G. *Phys. Rev. Lett.* **1999**, *83*, 5098−5101.

(8) Berber, S.; Kwon, Y.-K.; Tomanek, D. *Phys. Rev. Lett.* **2000**, *84*, 4613−4616.

(9) Coleman, J. N.; Khan, U.; Gun'ko, Y. K. *Adv. Mater.* **2006**, *18*, 689−706.

(10) Xie, X.-L.; Mai, Y.-W.; Zhou, X.-P. *Mater. Sci. Eng., R* **2005**, *R49*, 89−112.

(11) Thostenson, E. T.; Li, C.; Chou, T.-W. *Compos. Sci. Technol.* **2005**, *65*, 491−516.

(12) Miyagawa, H.; Misra, M.; Mohanty, A. K. *J. Nanosci. Nanotechnol.* **2005**, *5*, 1593−1615.

(13) Du, F.; Winey, K. I. In *Nanomaterials Handbook*; Gogotsi, Y., Ed.; CRC Press: Boca Raton, FL, 2006; pp 565−582.

(14) Awasthi, K.; Srivastava, A.; Srivastava, O. N. *J. Nanosci. Nanotechnol.* **2005**, *5*, 1616−1636.

(15) Monthioux, M. *Carbon* **2002**, *40*, 1809−1823.

(16) Thostenson, E. T.; Zhifeng, R.; Chou, T.-W. *Compos. Sci. Technol.* **2001**, *61*, 1899−1912.

(17) Dyke, C. A.; Tour, J. M. *J. Phys. Chem. A* **2004**, *108*, 11151−11159.

(18) Wang, N.; Li, G. D.; Tang, Z. K. *Chem. Phys. Lett.* **2001**, *339*, 47−52.

(19) Zheng, L. X.; O'Connell, M. J.; Doorn, S. K.; Liao, X. Z.; Zhao, Y. H.; Akhadov, E. A.; Hoffbauer, M. A.; Roop, B. J.; Jia, Q. X.; Dye, R. C.; Peterson, D. E.; Huang, S. M.; Liu, J.; Zhu, Y. T. *Nat. Mater.* **2004**, *3*, 673−676.

(20) Star, A.; Stoddart, J. F.; Steuerman, D.; Diehl, M.; Boukai, A.; Wong, E. W.; Yang, X.; Chung, S.-W.; Choi, H.; Heath, J. R. *Angew. Chem., Int. Ed.* **2001**, *40*, 1721−1725.

(21) Islam, M. F.; Rojas, E.; Bergey, D. M.; Johnson, A. T.; Yodh, A. G. *Nano Lett.* **2003**, *3*, 269−273.

(22) Bryning, M. B.; Islam, M. F.; Kikkawa, J. M.; Yodh, A. G. *Adv. Mater.* **2005**, *17*, 1186−1191.

(23) Du, F.; Fischer, J. E.; Winey, K. I. *Phys. Rev. B: Condens. Matter* **2005**, *72*, 121404/1−121404/4.

(24) Badaire, S.; Poulin, P.; Maugey, M.; Zakri, C. *Langmuir* **2004**, *20*, 10367−10370.

(25) Yurekli, K.; Mitchell, C. A.; Krishnamoorti, R. *J. Am. Chem. Soc.* **2004**, *126*, 9902−9903.

(26) Zhou, W.; Islam, M. F.; Wang, H.; Ho, D. L.; Yodh, A. G.; Winey, K. I.; Fischer, J. E. *Chem. Phys. Lett.* **2004**, *384*, 185−189.

(27) Wang, H.; Zhou, W.; Ho, D. L.; Winey, K. I.; Fischer, J. E.; Glinka, C. J.; Hobbie, E. K. *Nano Lett.* **2004**, *4*, 1789−1793.

(28) Schaefer, D. W.; Zhao, J.; Brown, J. M.; Anderson, D. P.; Tomlin, D. W. *Chem. Phys. Lett.* **2003**, *375*, 369−375.

(29) Bauer, B. J.; Hobbie, E. K.; Becker, M. L. *Macromolecules* **2006**, *39*, 2637−2642.

(30) Davis, V. A.; Ericson, L. M.; Parra-Vasquez, A. N. G.; Fan, H.; Wang, Y.; Prieto, V.; Longoria, J. A.; Ramesh, S.; Saini, R. K.; Kittrell, C.; Billups, W. E.; Adams, W. W.; Hauge, R. H.; Smalley, R. E.; Pasquali, M. *Macromolecules* **2004**, *37*, 154−160.

(31) Fry, D.; Langhorst, B.; Wang, H.; Becker, M. L.; Bauer, B. J.; Grulke, E. A.; Hobbie, E. K. *J. Chem. Phys.* **2006**, *124*, 054703/1−054703/9.

(32) Niyogi, S.; Hamon, M. A.; Hu, H.; Zhao, B.; Bhowmik, P.; Sen, R.; Itkis, M. E.; Haddon, R. C. *Acc. Chem. Res.* **2002**, *35*, 1105−1113.

(33) Georgakilas, V.; Kordatos, K.; Prato, M.; Guldi, D. M.; Holzinger, M.; Hirsch, A. *J. Am. Chem. Soc.* **2002**, *124*, 760−761.

(34) Sun, Y.-P.; Fu, K.; Lin, Y.; Huang, W. *Acc. Chem. Res.* **2002**, *35*, 1096−1104.

(35) Dyke, C. A.; Tour, J. M. *Chem.—Eur. J.* **2004**, *10*, 812−817.

(36) Star, A.; Liu, Y.; Grant, K.; Ridvan, L.; Stoddart, J. F.; Steuerman, D. W.; Diehl, M. R.; Boukai, A.; Heath, J. R. *Macromolecules* **2003**, *36*, 553−560.

(37) Du, F.; Scogna, R. C.; Zhou, W.; Brand, S.; Fischer, J. E.; Winey, K. I. *Macromolecules* **2004**, *37*, 9048−9055.

(38) Bellayer, S.; Gilman, J. W.; Eidelman, N.; Bourbigot, S.; Flambard, X.; Fox, D. M.; De Long, H. C.; Trulove, P. C. *Adv. Funct. Mater.* **2005**, *15*, 910−916.

(39) Chatterjee, T.; Yurekli, K.; Hadjiev, V. G.; Krishnamoorti, R. *Adv. Funct. Mater.* **2005**, *15*, 1832−1838.

(40) Barrau, S.; Demont, P.; Perez, E.; Peigney, A.; Laurent, C.; Lacabanne, C. *Macromolecules* **2003**, *36*, 9678−9680.

(41) Bryning, M. B.; Milkie, D. E.; Islam, M. F.; Kikkawa, J. M.; Yodh, A. G. *Appl. Phys. Lett.* **2005**, *87*, 161909/1−161909/3.

(42) Sundararajan, P. R.; Singh, S.; Moniruzzaman, M. *Macromolecules* **2004**, *37*, 10208−10211.

(43) De la Chapelle, M. L.; Stephan, C.; Nguyen, T. P.; Lefrant, S.; Journet, C.; Bernier, P.; Munoz, E.; Benito, A.; Maser, W. K.; Martinez, M. T.; De la Fuente, G. F.; Guillard, T.; Flamant, G.; Alvarez, L.; Laplaze, D. *Synth. Met.* **1999**, *103*, 2510−2512.

(44) Benoit, J. M.; Corraze, B.; Lefrant, S.; Blau, W. J.; Bernier, P.; Chauvet, O. *Synth. Met.* **2001**, *121*, 1215−1216.

(45) Singh, S.; Pei, Y.; Miller, R.; Sundararajan, P. R. *Adv. Funct. Mater.* **2003**, *13*, 868−872.

(46) Du, F.; Fischer, J. E.; Winey, K. I. *J. Polym. Sci., Part B: Polym. Phys.* **2003**, *41*, 3333−3338.

(47) Haggenmueller, R.; Fischer, J. E.; Winey, K. I. *Macromolecules* **2006**, *39*, 2964−2971.

(48) Poetschke, P.; Bhattacharyya, A. R.; Janke, A.; Goering, H. *Compos. Interfaces* **2003**, *10*, 389−404.

(49) Liu, T.; Phang, I. Y.; Shen, L.; Chow, S. Y.; Zhang, W.-D. *Macromolecules* **2004**, *37*, 7214−7222.

(50) Zhang, W. D.; Shen, L.; Phang, I. Y.; Liu, T. *Macromolecules* **2004**, *37*, 256−259.

(51) Bhattacharyya, A. R.; Sreekumar, T. V.; Liu, T.; Kumar, S.; Ericson, L. M.; Hauge, R. H.; Smalley, R. E. *Polymer* **2003**, *44*, 2373−2377.

(52) Siochi, E. J.; Working, D. C.; Park, C.; Lillehei, P. T.; Rouse, J. H.; Topping, C. C.; Bhattacharyya, A. R.; Kumar, S. *Composites, Part B* **2004**, *35B*, 439−446.

(53) Haggenmueller, R.; Gommans, H. H.; Rinzler, A. G.; Fischer, J. E.; Winey, K. I. *Chem. Phys. Lett.* **2000**, *330*, 219−225.

(54) Jin, Z.; Pramoda, K. P.; Goh, S. H.; Xu, G. *Mater. Res. Bull.* **2002**, *37*, 271−278.

(55) Schadler, L. S.; Giannaris, S. C.; Ajayan, P. M. *Appl. Phys. Lett.* **1998**, *73*, 3842−3844.

(56) Zhu, J.; Kim, J.; Peng, H.; Margrave, J. L.; Khabashesku, V. N.; Barrera, E. V. *Nano Lett.* **2003**, *3*, 1107−1113.

(57) Zhu, J.; Peng, H.; Rodriguez-Macias, F.; Margrave, J. L.; Khabashesku, V. N.; Imam, A. M.; Lozano, K.; Barrera, E. V. *Adv. Funct. Mater.* **2004**, *14*, 643−648.

(58) Gong, X.; Liu, J.; Baskaran, S.; Voise, R. D.; Young, J. S. *Chem. Mater.* **2000**, *12*, 1049−1052.

(59) Ajayan, P. M.; Schadler, L. S.; Giannaris, C.; Rubio, A. *Adv. Mater.* **2000**, *12*, 750−753.

(60) Moniruzzaman, M.; Du, F.; Romero, N.; Winey, K. I. *Polymer* **2006**, *47*, 293−298.

(61) Raravikar, N. R.; Schadler, L. S.; Vijayaraghavan, A.; Zhao, Y.; Wei, B.; Ajayan, P. M. *Chem. Mater.* **2005**, *17*, 974−983.

(62) Feng, W.; Bai, X. D.; Lian, Y. Q.; Liang, J.; Wang, X. G.; Yoshino, K. *Carbon* **2003**, *41*, 1551−1557.

(63) Du, F.; Guthy, C.; Kashiwagi, T.; Fischer, J. E.; Winey, K. I. *J. Polym. Sci., Part B: Polym. Phys.* **2006**, *44*, 1513−1519.

(64) Huang, H.; Liu, C.; Wu, Y.; Fan, S. *Adv. Mater.* **2005**, *17*, 1652−1656.

(65) Xia, H.; Wang, Q.; Li, K.; Hu, G.-H. *J. Appl. Polym. Sci.* **2004**, *93*, 378−386.

(66) Kasimatis, K. G.; Nowell, J. A.; Dykes, L. M.; Burghardt, W. R.; Thillalyan, R.; Brinson, L. C.; Andrews, R.; Torkelson, J. M. *PMSE Prepr.* **2005**, *92*, 255−256.

(67) Regev, O.; ElKati, P. N. B.; Loos, J.; Koning, C. E. *Adv. Mater.* **2004**, *16*, 248−251.

(68) Dufresne, A.; Paillet, M.; Putaux, J. L.; Canet, R.; Carmona, F.; Delhaes, P.; Cui, S. *J. Mater. Sci.* **2002**, *37*, 3915−3923.

(69) Vigolo, B.; Penicaud, A.; Coulon, C.; Sauder, C.; Pailler, R.; Journet, C.; Bernier, P.; Poulin, P. *Science* **2000**, *290*, 1331−1334.

(70) Mamedov, A. A.; Kotov, N. A.; Prato, M.; Guldi, D. M.; Wicksted, J. P.; Hirsch, A. *Nat. Mater.* **2002**, *1*, 190−194.

(71) Kimura, T.; Ago, H.; Tobita, M.; Ohshima, S.; Kyotani, M.; Yumura, M. *Adv. Mater.* **2002**, *14*, 1380−1383.

(72) Jin, L.; Bower, C.; Zhou, O. *Appl. Phys. Lett.* **1998**, *73*, 1197−1199.

(73) Safadi, B.; Andrews, R.; Grulke, E. A. *J. Appl. Polym. Sci.* **2002**, *84*, 2660−2669.

(74) Haggenmueller, R.; Zhou, W.; Fischer, J. E.; Winey, K. I. *J. Nanosci. Nanotechnol.* **2003**, *3*, 105−110.

(75) Ge Jason, J.; Hou, H.; Li, Q.; Graham Matthew, J.; Greiner, A.; Reneker Darrell, H.; Harris Frank, W.; Cheng Stephen, Z. D. *J. Am. Chem. Soc.* **2004**, *126*, 15754−15761.

(76) Gao, J.; Yu, A.; Itkis, M. E.; Bekyarova, E.; Zhao, B.; Niyogi, S.; Haddon, R. C. *J. Am. Chem. Soc.* **2004**, *126*, 16698−16699.

(77) Hou, H.; Ge, J. J.; Zeng, J.; Li, Q.; Reneker, D. H.; Greiner, A.; Cheng, S. Z. D. *Chem. Mater.* **2005**, *17*, 967−973.

(78) Ko, F.; Gogotsi, Y.; Ali, A.; Naguib, N.; Ye, H.; Yang, G.; Li, C.; Willis, P. *Adv. Mater.* **2003**, *15*, 1161−1165.

(79) Dalton, A. B.; Collins, S.; Munoz, E.; Razal, J. M.; Ebron, V. H.; Ferraris, J. P.; Coleman, J. N.; Kim, B. G.; Baughman, R. H. *Nature (London)* **2003**, *423*, 703.

(80) Agarwal, B. D.; Broutman, L. G. *Analysis and Performance of Fiber Composites.* Wiley: New York, 1980.

(81) Mallick, P. K. *Fiber-Reinforced Composites;* Marcel Dekker: New York, 1993.

(82) Barber, A. H.; Cohen, S. R.; Wagner, H. D. *Appl. Phys. Lett.* **2003**, *82*, 4140−4142.

(83) Liao, K.; Li, S. *Appl. Phys. Lett.* **2001**, *79*, 4225−4227.

(84) Lordi, V.; Yao, N. *J. Mater. Res.* **2000**, *15*, 2770−2779.

(85) Frankland, S. J. V.; Caglar, A.; Brenner, D. W.; Griebel, M. *J. Phys. Chem. B* **2002**, *106*, 3046−3048.

(86) Geng, H.; Rosen, R.; Zheng, B.; Shimoda, H.; Fleming, L.; Liu, J.; Zhou, O. *Adv. Mater.* **2002**, *14*, 1387−1390.

(87) Gao, J.; Itkis, M. E.; Yu, A.; Bekyarova, E.; Zhao, B.; Haddon, R. C. *J. Am. Chem. Soc.* **2005**, *127*, 3847−3854.

(88) Baughman Ray, H.; Zakhidov Anvar, A.; de Heer Walt, A. *Science* **2002**, *297*, 787−92.

(89) Ramasubramaniam, R.; Chen, J.; Liu, H. *Appl. Phys. Lett.* **2003**, *83*, 2928−2930.

(90) Sandler, J. K. W.; Kirk, J. E.; Kinloch, I. A.; Shaffer, M. S. P.; Windle, A. H. *Polymer* **2003**, *44*, 5893−5899.

(91) Bai, J. B.; Allaoui, A. *Composites, Part A* **2003**, *34A*, 689−694.

(92) Martin, C. A.; Sandler, J. K. W.; Shaffer, M. S. P.; Schwarz, M. K.; Bauhofer, W.; Schulte, K.; Windle, A. H. *Compos. Sci. Technol.* **2004**, *64*, 2309−2316.

(93) Li, S.; Qin, Y.; Shi, J.; Guo, Z.-X.; Li, Y.; Zhu, D. *Chem. Mater.* **2005**, *17*, 130−135.

(94) Ramanathan, T.; Liu, H.; Brinson, L. C. *J. Polym. Sci., Part B: Polym. Phys.* **2005**, *43*, 2269−2279.

(95) Tamburri, E.; Orlanducci, S.; Terranova, M. L.; Valentini, F.; Palleschi, G.; Curulli, A.; Brunetti, F.; Passeri, D.; Alippi, A.; Rossi, M. *Carbon* **2005**, *43*, 1213−1221.

(96) Valentini, L.; Armentano, I.; Puglia, D.; Kenny, J. M. *Carbon* **2004**, *42*, 323−329.

(97) Krishnamoorti, R.; Giannelis, E. P. *Macromolecules* **1997**, *30*, 4097−4102.

(98) Mitchell, C. A.; Bahr, J. L.; Arepalli, S.; Tour, J. M.; Krishnamoorti, R. *Macromolecules* **2002**, *35*, 8825−8830.

(99) Krishnamoorti, R.; Yurekli, K. *Curr. Opin. Colloid Interface Sci.* **2001**, *6*, 464−470.

(100) Poetschke, P.; Abdel-Goad, M.; Alig, I.; Dudkin, S.; Lellinger, D. *Polymer* **2004**, *45*, 8863−8870.

(101) Hough, L. A.; Islam, M. F.; Janmey, P. A.; Yodh, A. G. *Phys. Rev. Lett.* **2004**, *93*, 168102/1−168102/4.

(102) Zhong, H.; Lukes, J. R. *Proceedings of IMECE04 2004 ASME International Mechanical Engineering Congress and Exposition*, Anaheim, CA, Nov 13−20, 2004.

(103) Biercuk, M. J.; Llaguno, M. C.; Radosavljevic, M.; Hyun, J. K.; Johnson, A. T.; Fischer, J. E. *Appl. Phys. Lett.* **2002**, *80*, 2767−2769.

(104) Choi, E. S.; Brooks, J. S.; Eaton, D. L.; Al-Haik, M. S.; Hussaini, M. Y.; Garmestani, H.; Li, D.; Dahmen, K. *J. Appl. Phys.* **2003**, *94*, 6034−6039.

(105) Huxtable, S. T.; Cahill, D. G.; Shenogin, S.; Xue, L.; Ozisik, R.; Barone, P.; Usrey, M.; Strano, M. S.; Siddons, G.; Shim, M.; Keblinski, P. *Nat. Mater.* **2003**, *2*, 731−734.

(106) Hone, J.; Llaguno, M. C.; Nemes, N. M.; Johnson, A. T.; Fischer, J. E.; Walters, D. A.; Casavant, M. J.; Schmidt, J.; Smalley, R. E. *Appl. Phys. Lett.* **2000**, *77*, 666−668.

(107) Gojni, F. H.; Wichmann, M. H. G.; Fiedler, B.; Kinloch, I. A.; Bauhofer, W.; Windle, A. H.; Schulte, K. *Polymer* **2006**, *47*, 2036−2045.

(108) Shenogin, S.; Bodapati, A.; Xue, L.; Ozisik, R.; Keblinski, P. *Appl. Phys. Lett.* **2004**, *85*, 2229−2231.

(109) Liu, C. H.; Fan, S. S. *Appl. Phys. Lett.* **2005**, *86*, 123106/1−123106/3.

(110) Beyer, G. *Fire Mater.* **2002**, *26*, 291−293.

(111) Kashiwagi, T.; Du, F.; Douglas, J. F.; Winey, K. I.; Harris, R. H.; Shields, J. R. *Nat. Mater.* **2005**, *4*, 928−933.

(112) Kashiwagi, T.; Du, F.; Winey, K. I.; Groth, K. M.; Shields, J. R.; Bellayer, S. P.; Kim, H.; Douglas, J. F. *Polymer* **2005**, *46*, 471−481.

(113) Dyke, C. A.; Tour, J. M. *Nano Lett.* **2003**, *3*, 1215−1218.

(114) Liang, F.; Sadana, A. K.; Peera, A.; Chattopadhyay, J.; Gu, Z.; Hauge, R. H.; Billups, W. E. *Nano Lett.* **2004**, *4*, 1257−1260.

(115) Graff, R. A.; Swanson, J. P.; Barone, P. W.; Baik, S.; Heller, D. A.; Strano, M. S. *Adv. Mater.* **2005**, *17*, 980−984.

(116) Chattopadhyay, D.; Galeska, I.; Papadimitrakopoulos, F. *J. Am. Chem. Soc.* **2003**, *125*, 3370−3375.

(117) Gelves, G. A.; Sundararaj, U.; Haber, J. A. *Macromol. Rapid Commun.* **2005**, *26*, 1677−1681.